Anisotropic Ferromagnetism in Substituted Zinc Oxide

M. Venkatesan, C. B. Fitzgerald, J. G. Lunney, and J. M. D. Coey

Physics Department, Trinity College, Dublin 2, Ireland

Room-temperature ferromagnetism is observed in (110) oriented ZnO films made from targets containing 5 at.% of Sc, Ti, V, Fe, Co, or Ni, but not Cr, Mn, or Cu ions. There are large moments, $2.6\mu_B$ and $0.5\mu_B$/dopant atom for Co- and Ti-containing oxides, respectively. There is also a moment of $0.3\mu_B$/Sc. Magnetization is very anisotropic, with variations of up to a factor of 3 depending on the orientation of the applied field relative to the substrate. Results are interpreted in terms of a spin-split donor impurity-band model, which can account for ferromagnetism in insulating or conducting high-k oxides with concentrations of magnetic ions that lie far below the percolation threshold. Magnetic moments are associated with two-electron defects in the films as well as unpaired electrons of the $3d$ ions.

         PACS numbers: 75.50.Pp, 75.10.–b, 75.30.Gw, 75.30.Hx

Ferromagnetism in dilute magnetic oxides is the most interesting new problem in magnetism to emerge so far this century. Following the original report by Ueda *et al.* [1], there have been sporadic but inconsistent reports that thin films of the wide-gap semiconductor ZnO exhibit ferromagnetism with a Curie point above room temperature when a few atomic percent of cobalt [2–6] or another transition element [7–11] is substituted for zinc. The results are sensitive to the form of the sample and preparation method. Other studies found lower magnetic ordering temperatures [12–15] or no ferromagnetism at all above 4 K for any $3d$ dopant [16]. In the absence of an evident exchange mechanism which could account for a high Curie temperature at doping levels far below the percolation threshold, these reports were received with skepticism and the belief that the ferromagnetism must somehow be associated with clustering or incipient formation of secondary phases. Nevertheless, there is good spectroscopic evidence that divalent cobalt does indeed substitute on the tetrahedral sites of the wurtzite structure [1,12,17–19], with a wide solid solubility range [15]. Searches by Rode *et al.* [4] and Ramachandran *et al.* [19] revealed no evidence for phase segregation in Co-doped ZnO films. But, until a clear connection between the magnetic properties and electronic structure can be established, doubts that doped zinc oxide is truly a magnetic semiconductor will persist.

We recently proposed a model for high-temperature ferromagnetism in dilute magnetic semiconductors, where the exchange is mediated by carriers in a spin-split impurity band derived from extended donor orbitals [20]. The model associates bound magnetic polarons with the electrons in extended Bohr orbits of radius γa_0 surrounding the defects in a high-k dielectric. Here a_0 is the Bohr radius and γ is defined as $k m_e/m^*$, where k is the high-frequency dielectric constant and m^* is the electron effective mass; the value of γ for ZnO is 14. The model predicts ferromagnetism at the polaron percolation threshold, when the carrier concentration per cation δ

exceeds $4.3/\gamma^3$. To avoid antiferromagnetic ordering, the concentration of magnetic cations x must lie below the cation nearest-neighbor percolation threshold x_c, which is ≈ 0.17 for the wurtzite structure. The Curie temperature for substituted ZnO in the molecular field approximation is given by the expression

$$T_c = 0.04[\delta x S(S + 1)]^{1/2} J_{sd}/k_B, \qquad (1)$$

where x is the atomic concentration of substituent cations with spin S and J_{sd} is the exchange coupling with the impurity band. Higher Curie temperatures are expected only when $3d$ states of the transition element hybridize with the spin-split impurity-band states at the Fermi level, providing transfer from the impurity band to the $3d$ ion of 0.01–0.02 electrons per cation.

In order to probe the origin of the high-temperature ferromagnetism in $(Zn_{1-x}M_x)O$, we have examined the systematic variation of the magnetism (i) as a function of transition-metal M at fixed concentration $x = 5\%$, (ii) as a function of transition-metal concentration and film thickness for $M = Co$, and (iii) as a function of oxygen pressure during film growth for $x = 5\%$ and $M = Co$.

All samples were prepared by conventional pulsed-laser deposition using a KrF excimer laser operating at 248 nm and a fluence of $1.8\ J\,cm^{-2}$. Targets were prepared by standard ceramic procedures from ZnO and MO or M_2O_3 powders of $4N$ purity. The substrates were $5 \times 5\ mm^2$ R-cut ($1\bar{1}02$) sapphire maintained at $600\ ^\circ C$. The oxygen pressure during deposition was varied from 1 to 10^{-4} mbar. Film thickness was in the range 60–120 nm. It was measured with a precision of $\pm 10\%$ using an *in situ* optical reflectivity monitor during deposition and checked by small-angle x-ray reflectivity measurements. The films are transparent and strongly textured, showing only the (110) reflection of the wurtzite structure. Film composition was determined by energy dispersive x-ray analysis for a series of nine cobalt films prepared from targets with nominal composition x' ranging from 0.01 to 0.15. The relation between x' and x is almost linear, with x

     0031-9007/04/93(17)/177206(4)$22.50   © 2004 The American Physical Society

being about 30% greater than x' [21]. For the light transition-metal dopants x was as much as $3x'$.

Substitution of cobalt cations in the tetrahedral sites of the wurtzite structure was confirmed by optical spectroscopy. A series of characteristic optical absorption bands in the infrared and in the visible have been identified with d-d transitions of the high-spin Co^{2+} $3d^7$ ^4F ion in tetrahedral oxygen coordination [22,23]. The absorption in the visible was thought to derive from the $^4A_2 \rightarrow$ $^4T_1(^4P)$ and $^4A_2 \rightarrow$ $^2E(^2G)$ transitions, and those in the infrared from the $^4A_2 \rightarrow$ $^4T_1(^4F)$ transition. The orbital triplet final states are split into a singlet and a doublet by the trigonal component of the crystal field at the tetrahedral site, which has $3m$ symmetry. The strength of these absorption bands scales with the cobalt content of our films [21].

The variation of the magnetic moment across the nominal $(Zn_{0.95}M_{0.05})O$ series is illustrated in Fig. 1. Measurements were made in a Quantum Design MPMS-XL SQUID magnetometer using linear regression and no autotracking. There is a striking systematic variation, with maxima near the beginning of the $3d$ series at Ti and V ($0.5\mu_B$), and towards the end of the series at Co ($1.9\mu_B$) when the field is applied perpendicular to the film. No moment appreciably greater than the experimental uncertainty ($< 0.1\mu_B$) was observed at room temperature for Cr, Mn, Cu, or Zn. The other ions, including scandium, exhibit smaller moments. Ferromagnetism in Sc-doped ZnO is quite a surprise, since neither Zn^{2+} ($3d^{10}$) nor Sc^{3+} ($3d^0$) are magnetic ions, and the $3d$ level of zinc lies well below that of scandium [24], so no electron transfer to scandium is envisaged.
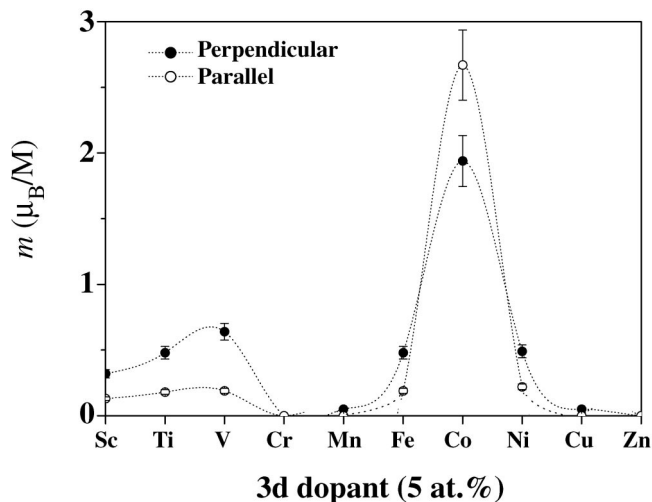
Another surprise is the huge anisotropy of the magnetization. This has been measured for Sc, Ti, V, Fe, Co, and Ni. Data for Co are presented in Fig. 2. The $^4A_2$ ground state of Co^{2+} has no orbital angular momentum. In every case except cobalt, the moment is greatest when the field is applied perpendicular to the plane of the film, similar to the anisotropic d^0 ferromagnetism recently discovered in unsubstituted HfO_2 [25]. In addition, some of the ZnO films on R-cut sapphire show an enormous in-plane anisotropy, with twofold and fourfold symmetry. The moment per cobalt varies from $0.8\mu_B$ to $2.6\mu_B$ in the plane, with the largest value measured with the field parallel to the edge of the substrate, and the smallest along a diagonal which coincides with the c axis of ZnO films. The ZnO c axis lies parallel to the substrate $[12\bar{1}]$ axis [26].

More data for the cobalt-containing ZnO are shown in Fig. 3. The samples with 5 at.% Co prepared at different oxygen pressures are n-type conductors when the oxygen pressure is less than 0.1 mbar, and insulators ($\rho > 10\,\Omega$ m) at greater pressure. The carriers in ZnO are associated with oxygen vacancies or interstitial zinc atoms [27,28]. The data in Fig. 3(a) show that the ferromagnetism is destroyed as the carriers and their associated defects are eliminated.

Figure 3(b) shows how the average cobalt moment in films prepared at 10^{-4} mbar varies with cobalt concentration. The low-concentration limit is $m \approx 5.5\mu_B/Co$, compared to the spin-only moment $m_{spin} = 3\mu_B$ of high-spin Co^{2+} ($e^4t_2^3$). The falloff in moment with increasing x can be rationalized in terms of cobalt ions with their spin-only moment, randomly distributed over the cation sites in the wurtzite lattice. Isolated ions contribute the full moment m, pairs and most groups of four are
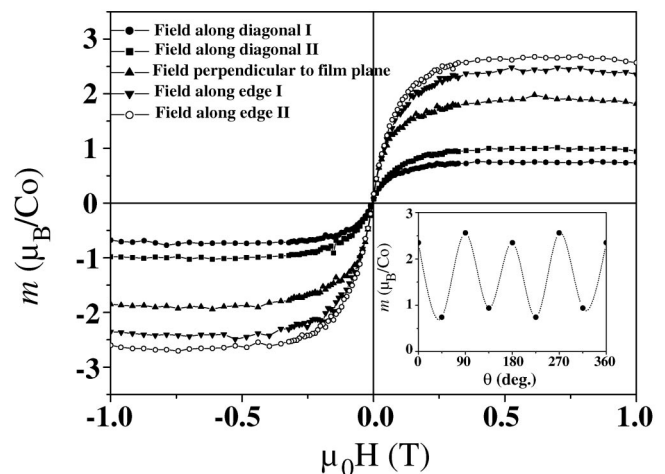

FIG. 1. Magnetic moment of $(Zn_{1-x}M_x)O$ films, $M =$ Sc, Ti, ..., Cu, Zn, measured at room temperature. Solid circles are for the field applied perpendicular to the film plane and open circles are for the field applied in the plane of the film. The moment is expressed as μ_B/M. The trend measured at 5 K is similar.

FIG. 2. Magnetization curves of a $(Zn_{0.93}Co_{0.07})O$ film with the magnetic field applied perpendicular to the plane of the film, or in plane in different directions. The in-plane anisotropy is shown in the inset. Data are corrected for the diamagnetism of the substrate, -0.20×10^{-12} m^3.

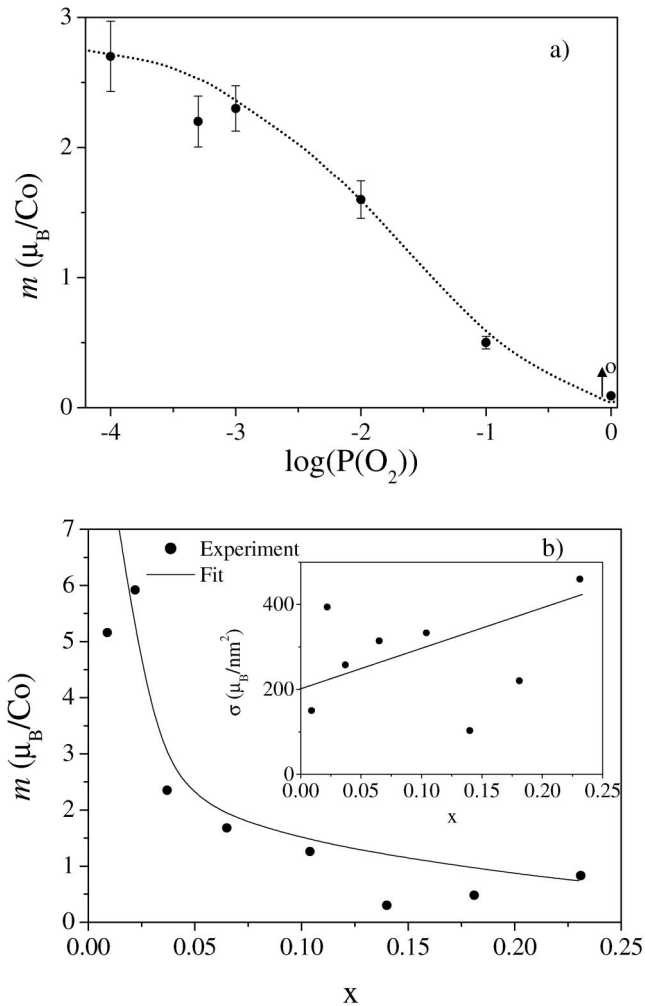FIG. 3. (a) Magnetic moment of $(Zn_{0.93}Co_{0.07})O$ measured at room temperature for films prepared at different oxygen pressures (the open symbol is for a film after annealing at 700 °C in vacuum). (b) Magnetic moment of $(Zn_{1-x}Co_x)O$ measured at room temperature for films prepared at 10^{-4} mbar for different x. The solid line is based on a weighted random distribution of cobalt ions over the cation sites of the wurtzite lattice, with strong antiferromagnetic coupling of nearest-neighbor cobalt cations and a constant contribution due to defects. The inset shows how the constant contribution is deduced by extrapolating the magnetic moment to $x = 0$.

antiferromagnetically coupled and make no net contribution, and triplets contribute $m/3$. Large antiferromagnetically coupled clusters of N atoms will make a contribution $m/N^{1/2}$. An additional moment described below has to be included. The model reproduces the trend in Fig. 3(b), provided the zinc distribution is slightly weighted in favor of transition-metal nearest-neighbor pairs.

The variation of magnetic moment across the series shown in Fig. 1 is as expected from the spin-split impurity-band model [20], which can account for ferromagnetism in high-k dielectrics doped with a few percent

of transition-metal ions. For the light $3d$ elements, the $3d^{\uparrow}$ states lie high in the $2p(O) - 4s(Zn)$ gap, overlapping the donor impurity band which is spin split as shown in Fig. 4. In the middle of the series, there is no overlap with the $3d$ levels and exchange is weak, but towards the end of the series the $3d^{\downarrow}$ states overlap the impurity band, which then has the opposite spin splitting for the same occupancy. High Curie temperatures are found whenever unoccupied $3d$ states overlap the impurity band, but not otherwise. The likely origin of the donor impurity band in ZnO films is lattice defects, such as oxygen vacancies, which have trapped between one and two electrons (F^0 centers) [27,28].

The valence of the substitutional $3d$ ions changes at some point along the series. Cobalt is divalent; titanium is trivalent. Iron can have either valence depending on the preparation conditions. Divalent cations simply replace zinc, but trivalent ones also act as electron dopants or else they create zinc vacancies (V^0 centers). However, there is no obvious correlation between conductivity and cation valence (Ti, Cr, and Fe are insulating, and the others are conducting) or conductivity and magnetism. The electrons in the impurity band will be localized by the influence of electronic correlations and potential fluctuations [29] associated with the dopant cations. Localization does not preclude ferromagnetic coupling, providing the localization length is not much shorter than γa_0.

The huge anisotropy of the magnetization of the oriented films and the large moment per cobalt ion at low concentrations are very unusual, and probably related. Giant moments were first reported by Ogale et al. for SnO_2 doped with Co [30], and later confirmed for Mn, Fe, and Co doping [31]. In view of the optical evidence for high-spin cobalt with a quenched orbital moment, we require another source of magnetism to account for the large moments in the dilute limit, as well as the magnetism produced by Sc^{3+}, which has no unpaired electrons. Two-electron defects such as F_t centers (an adjacent pair of F centers) for which a low-lying triplet state could be
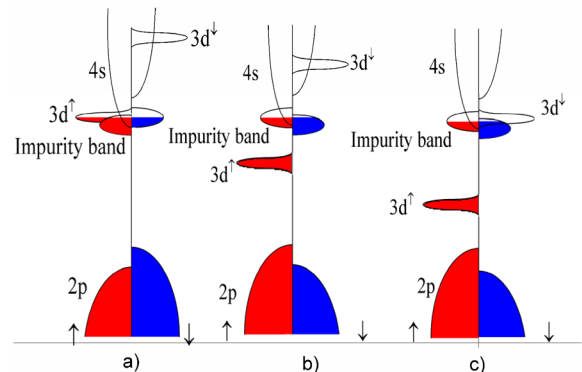

FIG. 4 (color online). Schematic density of states for (a) $M = $ Ti, (b) $M = $ Mn, and (c) $M = $ Co. The Fermi level lies in a spin-split donor impurity band.

stabilized by exchange with cobalt or V^0 centers (cation vacancies) which may have a triplet ground state [32] are good candidates. Extrapolating the moment in Fig. 3(b) to $x = 0$ gives a moment per unit substrate area of about $200\mu_B$ nm^{-2}, a magnitude we find in the Sc-doped ZnO and in other d^0 ferromagnets, such as HfO$_2$ [25]. Since ZnO films are not ferromagnetic, the defects in Co-doped ZnO, for example, must be "switched on" by Co, which suggests F_t centers, but this cannot be the case for Sc-ZnO, where Sc^{3+} introduces zinc vacancies; the V^0 center already has a triplet ground state in ZnO [32]. A calculation by Elfimov et al. for CaO indicates that these centers order ferromagnetically [33]. Anion vacancies can behave similarly [34].

The data in Fig. 1 indicate an anisotropic contribution to the magnetization unlike that expected of the 3d cation because the sign of the anisotropy does not follow the quarter-shell rule, changing sign with the quadrupole moment of the 3d shell. The anisotropy must somehow arise from an orbital moment associated with the molecular orbitals around oriented magnetic point defects.

In conclusion, the high-temperature ferromagnetism in doped zinc oxide films is an intriguing physical phenomenon, which differs from any previously known ferromagnetism or ferrimagnetism in oxides; it appears far below the percolation threshold and is highly anisotropic in a way that does not reflect the quadrupole moment of the 3d charge distribution. We find a connection between the electronic structure of $(Zn_{1-x}M_x)O$ and its ferromagnetic properties, which is understandable in terms of the spin-split donor impurity-band model. Secondary phases cannot be the explanation of the ferromagnetism, especially when $M =$ Sc or Ti. We have suggested a new source of magnetism in these oxides, namely, triplet states associated with two-electron defects. Electronic structure calculations are needed to study the role of the different defects and evaluate the associated orbital moments and the d character acquired by the impurity band. Predictions regarding the sign of the spin splitting at the bottom of the conduction band and the nature of the orbital moment should be investigated by measurements of magnetic dichroism.

[1] K. Ueda, H. Tabata, and T. Kawai, Appl. Phys. Lett. **79**, 988 (2001).

[2] Y. M. Cho, W. K. Choo, H. Kim, D. Kim, and Y. E. Ihm, Appl. Phys. Lett. **80**, 3358 (2001).

[3] H. J. Lee, S. Y. Jeong, C. R. Cho, and C. H. Park, Appl. Phys. Lett. **81**, 4020 (2002).

[4] K. Rode et al., J. Appl. Phys. **93**, 7676 (2003).

[5] W. Prellier, A. Fouchet, B. Mercey, C. Simon, and B. Raveau, Appl. Phys. Lett. **82**, 3490 (2003).

[6] D. P. Norton et al., Appl. Phys. Lett. **83**, 5488 (2003).

[7] H. Saeki, H. Tabata, and T. Kawai, Solid State Commun. **120**, 439 (2001).

[8] S. J. Han et al., Appl. Phys. Lett. **81**, 4212 (2002).

[9] P. Sharma et al., Nature Materials **2**, 673 (2003).

[10] P. V. Radovanovic and D. R. Gamelin, Phys. Rev. Lett. **91**, 157202 (2003).

[11] Y. W. Heo et al., Appl. Phys. Lett. **84**, 2292 (2004).

[12] K. Ando et al., Appl. Phys. Lett. **78**, 2700 (2001).

[13] T. Fukumura et al., Appl. Phys. Lett. **78**, 958 (2001).

[14] S. W. Jung et al., Appl. Phys. Lett. **80**, 4561 (2002).

[15] D. P. Norton et al., Appl. Phys. Lett. **82**, 239 (2003).

[16] Z. W. Jin et al., Appl. Phys. Lett. **78**, 3824 (2001).

[17] K. J. Kim and Y. R. Park, Appl. Phys. Lett. **81**, 1420 (2001).

[18] D. A. Schwartz, N. S. Norberg, Q. P. Nguyen, J. M. Parker, and D. M. Gamelin, J. Am. Chem. Soc. **125**, 13 205 (2003).

[19] S. Ramachandran, A. Tiwari, and J. Narayan, Appl. Phys. Lett. **84**, 5255 (2004).

[20] J. M. D. Coey, M. Venkatesan, and C. B. Fitzgerald (unpublished).

[21] C. B. Fitzgerald, M. Venkatesan, J. G. Lunney, L. S. Dorneles, and J. M. D. Coey, Appl. Surf. Sci. (to be published).

[22] P. Koidl, Phys. Rev. B **15**, 2493 (1977).

[23] S. W. Lim, D. K. Hwang, and J. M. Myoung, Solid State Commun. **125**, 231 (2003).

[24] J. A. Wilson, Adv. Phys. **21**, 143 (1972).

[25] M. Venkatesan, C. B. Fitzgerald, and J. M. D. Coey, Nature (London) **430**, 630 (2004).

[26] Y. Yoshino, K. Inoue, M. Takeuchi, and K. Ohwada, Vacuum **51**, 601 (1998).

[27] A. P. Roth, J. B. Webb, and D. F. Williams, Phys. Rev. B **25**, 7836 (1982).

[28] A. F. Kohan, G. Ceder, D. Morgan, and C. G. Van de Walle, Phys. Rev. B **61**, 15 019 (2000); S. B. Zhang, S. H. Wei, and A. Zunger, Phys. Rev. B **63**, 075205 (2001).

[29] N. F. Mott, Conduction in Noncrystalline Materials (Oxford University Press, New York, 1987).

[30] S. B. Ogale et al., Phys. Rev. Lett. **91**, 077205 (2003).

[31] C. B. Fitzgerald, M. Venkatesan, and J. M. D. Coey (unpublished).

[32] A. M. Stoneham, Theory of Defects in Solids (Clarendon Press, Oxford, 1975).

[33] I. S. Elfimov, S. Yunoki, and G. A. Sawatzky, Phys. Rev. Lett. **89**, 216403 (2002).

[34] R. Monnier and B. Delley, Phys. Rev. Lett. **87**, 157204 (2001).